9th U. S. National Combustion Meeting
Organized by the Central States Section of the Combustion Institute
May 17-20, 2015
Cincinnati, Ohio

Soot Formation and its Impact on Flame Radiation during Turbulent, Non-Premixed Oxygen-Enriched Combustion of Methane

Christopher R. Shaddix and Timothy C. Williams*

Combustion Research Facility
Sandia National Laboratories
7011 East Ave., Livermore, CA USA

**corresponding author: crshadd@sandia.gov*

Abstract: Non-premixed oxy-fuel combustion of natural gas is used in many important industrial applications where high-intensity heat is required, such as glass manufacturing and metal forging and shaping. In these applications, the high flame temperatures achieved by oxy-fuel increases radiative heat transfer to the surfaces of interest and soot formation within the flame is desired for further augmentation of radiation. However, the high energy consumption and overall economics of oxygen production have limited the penetration of oxy-fuel combustion technologies. New approaches to oxygen production, using ion transport membranes or metal organic frameworks (MOFs), are being developed which may reduce the oxygen production costs associated with conventional cryogenic air separation, but which are likely to be more economical for intermediate levels of oxygen enrichment of air, rather than for the nearly complete oxygen separation that occurs with cryogenic separation. To determine the influence of intermediate levels of oxygen enrichment on soot formation and radiation, we have developed a non-premixed coannular burner in which oxygen concentrations and flow rates are independently varied, in an attempt to separate the effects of turbulent mixing intensity, characteristic flame residence time, and oxygen enrichment on soot formation and flame radiation intensity. Local radiation intensities and soot concentrations have been measured using a thin-film thermopile and laser-induced incandescence, respectively. Results show that turbulence intensity has a marked effect on both soot formation and flame radiation. Somewhat surprisingly, soot formation is seen to increase as the oxygen concentration falls from 100%, for flames in which the turbulence intensity stays the same. Coincidentally, the thermal radiation from such flames with constant mixing intensity stays constant for an extended range of oxygen concentrations before gradually decreasing. These results suggest that properly designed oxygen-enriched burners may be able to achieve virtually identical thermal radiation intensities as traditional oxy-fuel burners utilizing high-purity oxygen.

Keywords: soot, radiation, oxy-fuel, turbulent, methane

1. Introduction

Oxygen-enriched combustion or pure oxy-fuel combustion are well-known approaches to improve the heat transfer associated with stationary energy processes utilized by industry and power production [1.2]. The addition of oxygen results in higher thermal efficiency, greater flame stability, improved ignition characteristics, greater burner turndown ratio, improved fuel flexibility, and reduced exhaust gas volumes, all stemming from the reduction or elimination of the N_2 component of air. In addition, NOx emissions can nearly be completely eliminated in pure

oxy-fuel combustion. Furthermore, oxygen-enriched or oxy-fuel combustion provides a lower-cost route to CO_2 capture, for either subsequent utilization (such as in enhanced oil recovery) or geologic sequestration [2].

The major advantage of oxygen-enriched or oxy-fuel combustion to thermal processes is through the much greater radiant emission from these flames. The radiant emission increases because of the higher flame temperatures associated with oxygen-enrichment and because the flame gases themselves have a much greater emissivity. The peak flame temperature during oxy-fuel combustion of natural gas is nearly 3000 K, compared to a peak temperature during air-firing of less than 2200 K. Absent the dilution from N_2 associated with traditional air-based combustion, the concentrations of combustion products CO_2 and steam (both of which are radiantly active) in oxy-fuel flames are 3.5 times larger than in air-fuel flames. Furthermore, careful tailoring of non-premixed oxygen-enriched or oxy-fuel flames allows the formation of enhanced soot levels within the flame, thereby further increasing the thermal radiation (while still continuing to burn the soot out within the flame brush and therefore avoiding soot emissions). As a result, 98% of the heat transfer from oxy-fuel flames to the 'batch' (the solid particle components that will make up the glass) in glass-melting furnaces has been shown to be through radiation [1]. Improvements in furnace efficiency when retrofitting air-fired furnaces to oxy-fired have ranged from 20-60% in glass and steel heating furnaces [3-5].

While the glass, aluminum, and steel industries have adopted oxy-fuel combustion into some of their operations, the overall penetration of oxy-fuel technology into industrial and power markets is currently constrained by the relatively high cost of existing air separation technologies for generating oxygen. Cryogenic air separation is the most widely used technology for generating oxygen at a large scale [6,7]. This approach generates oxygen with a purity of 90-99.5%, and can scale to large production sizes. Unfortunately it is a complex and expensive technology, in terms of both capital cost and energy consumption. Pressure swing adsorption (PSA) is a competing technology for relatively small-scale applications that do not require an oxygen purity greater than 94%. Current PSA systems rely on preferential adsorption of N_2 onto zeolytes and consist of a multi-step batch production process [6-9].

New advances in materials science offer the promise of lower-cost production of O_2 or of oxygen-enriched air through air separation via membranes (e.g. ion-transport membranes [10,11]) or through adsorption/PSA approaches with novel materials. Recently, a new class of materials known as metal-organic frameworks (MOFs) has been developed which can create very large surface areas as well as open metal coordination sites for gas adsorption [12]. Some preliminary studies of MOFs for air separation have been conducted, and, recently, work at Sandia National Laboratories has identified promising MOFs structure and compositions for improved air separation [13,14]. Ultimately, use of advanced MOFs or entirely new materials may allow cost-effective air-separation at near-ambient temperatures.

With the active research being performed on development of low-cost air separation, the question naturally arises as to what level of oxygen enrichment is necessary to achieve the desired benefits in the various industrial oxy-fuel applications. For those applications driven by CO_2 capture, the necessary O_2 concentration is likely to be quite high, because otherwise a significant exhaust gas purification system will need to be employed to increase the

concentration of CO_2 in the exhaust. However, for oxy-fuel systems driven by enhanced heat transfer, generating high-purity O_2 is probably not necessary. Consequently, an important question of practical relevance to the process industries is how much enhancement in radiative heating is possible with oxygen-enriched combustion at different levels of oxygen enrichment. Related to this question is how to design oxygen-enriched burners to maximize radiant emission. The presence of soot within a flame is known to enhance radiant heat transfer, potentially to a significant extent. The relationship between turbulent mixing, soot formation, and flame radiation in oxygen-enriched methane flames has not been previously explored in any real depth. Baukal and Gebhart [15] varied O2 levels from 25% to 100% in a diffusion flame burner firing natural gas over a variety of injection rates, from laminar to turbulent and measured the thermal radiation. Wang et al. [16] studied the NOx formation, mean soot formation, and thermal radiation from a series of natural gas and propane flames formed by injecting turbulent fuel jets into laminar oxidizer streams consisting of 21% to 100% O_2.

Here, we intend to expand upon Wang's study by utilizing more realistic turbulent flows of both methane fuel and oxidizer and to make detailed, spatially resolved measurements of both radiation and soot concentrations, through the use of a narrow-angle radiometer and full 2-D soot concentrations as measured via laser-induced incandescence.

2. Methods / Experimental

For this investigation a coannular (tube-in-tube) burner geometry was selected in which the fuel tube is a 3/16" smooth, seamless stainless steel tube and it is surrounded by a 3/8" smooth, seamless stainless steel tube in which the supplied oxygen flows. Both tubes have 0.028" wall thickness. These tube sizes yield a fuel tube internal diameter (ID) of 3.34 mm and an oxidizer tube ID of 8.10 mm. Both tubes are straight-cut at the end and are aligned so that they have a common injection end-plane (i.e. the fuel tube is neither recessed nor protrudes past the oxidizer tube).

An initial study was performed in which a stoichiometric amount of oxidizer was supplied through the annulus as the oxygen concentration was varied from 50% O_2 (balance of N_2) to 100% O_2. Providing a stoichiometric amount of oxidizer corresponds to practical industrial practice wherein little to no excess oxygen is supplied to the burner when using strongly oxygen-enriched air (because any oxygen in the exhaust represents wasted energy and cost). However, in this test series (referred herein as 'Series 1'), as the oxygen concentration in the oxidizer decreased, the volumetric flow rate of oxidizer necessarily increased, resulting in more rapid mixing of the fuel and oxidizer streams and reduced soot concentrations and flame lengths. Consequently, a second series of flames was investigated in which the fuel and oxidizer flow rates remained constant and the overall stoichiometry of the supplied gases varied with changes in the oxidizer concentration. For this series of flames ('Series 2'), the oxidizer flow rate was chosen such that a stoichiometric amount of oxidizer was present when 100% O2 was utilized, and for the cases with lower oxygen concentrations a substoichiometric amount of oxidizer was supplied. However, as these flames were formed in the open air, they naturally mixed in enough of the surrounding air to complete combustion of the fuel.

A methane flow rate of 18.5 standard liters per minute (slpm) was used for all flames, giving an injection velocity of 36 m/s and a Reynolds number of 7300, based on the fuel tube diameter.

The oxidizer flow rates varied from 37.0 slpm (100% O_2 in Series 1, and all flames in Series 2) to 74.0 slpm (50% O_2 in Series 1), corresponding to injection velocities of 18.3 to 36.5 m/s and Reynolds numbers from 3950 to 7890. All flow rates were controlled via mass flow controllers that had been calibrated with laminar flow elements.

Figure 1 shows photographs of a few of the flames that were investigated. The visible flame heights of the Series 2 flames (and the 100% O_2 case of Series 1) were approximately 450 mm.

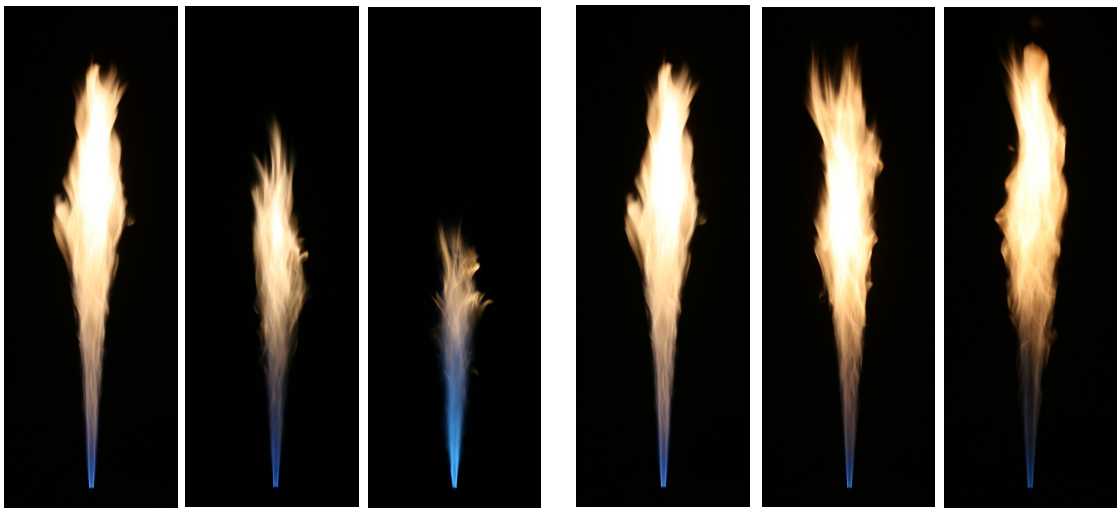

Figure 1: Photographs of oxygen-enriched flames for the stated oxygen concentrations. Series 1 flames provided stoichiometric oxygen (at different oxidizer flow rates), whereas Series 2 flames had a constant oxidizer flow rate (but different supplied gas stoichiometries). All photographs were taken with the same camera exposure, except for the 50% O_2 Series 1 flame, which has 4X the camera exposure of the other photographs.

Thermal radiation measurements were performed with a thin-film thermopile with a CaF_2 window. The use of the CaF_2 window material makes the radiometer equally sensitive to radiant emission from 0.13–11 μm, encompassing nearly all of the energy-containing radiation from the flame. The thermopile is 1 mm in diameter and has a characteristic response time of 32 ms. A black-anodized, 100 mm long steel tube with an ID of 3 mm minimizes light reflections within the probe and restricts incident radiation to a solid angle (Ω) of 1.61×10^{-3} sr. The detector sensor is located 250 mm away from the burner centerline, such that the detector measures radiation originating from within a cone with a base of 9 mm at the flame centerline. During experiments, the burner is traversed axially or radially to measure radiation along different paths. The radiometer signal was recorded using LABVIEW in 4 second duration time records captured at 500 samples/s. Each data record was then processed to calculate a mean, time-averaged signal.

Laser-induced incandescence (LII) measurements were performed using a Nd:YAG laser operating at a 10 Hz repetition rate with a pulse duration of approximately 9 ns. The laser output

was attenuated to 52 mJ/pulse using a ½-wave plate and glan laser polarizer. A power meter was used to assure constant laser pulse energy before and after each series of measurements. The 1064 nm beam was formed into a vertical sheet using a 1000 mm focal length bi-convex spherical lens in combination with a -200 nm focal length plano-concave cylindrical lens. The sheet height was 37 mm and the sheet thickness through the flame was 300 μm. The laser fluence was 0.47 J/cm^2, which was verified to be in the nominal 'plateau' region for making LII measurements with low sensitivity to variations in laser fluence. The laser sheet was positioned on the centerline of the flame and vertical traversing of the burner was used to move the measurement height. LII signals were detected using a Princeton Instruments PI-MAX fast-gating intensified CCD camera with a HQf GEN III intensifier and a CCD consisting of 512x512 pixels. The intensifier gate width was set to 100 ns with the center of the laser pulse arriving 16 ns after the onset of gate opening. A 600 nm low-pass filter was attached to the camera lens to minimize contributions from natural flame luminosity. 1000 images were collected at each measurement location, together with 250 images of background signal with the laser turned off. Examination of the single-shot images confirmed that the signal intensities were low enough that nonlinear effects associated with high signal counts were negligible. Figure 2 shows two sample images of LII signals collected from the flame with 100% O_2. The 1000 signal images were averaged at each location to form a mean signal image, from which the corresponding mean background image was subtracted. To characterize the soot concentrations in the different flames, a central square region of 7.75 mm on a side was analyzed in the center of each mean data image to compute a characteristic soot intensity at that location in the flame.

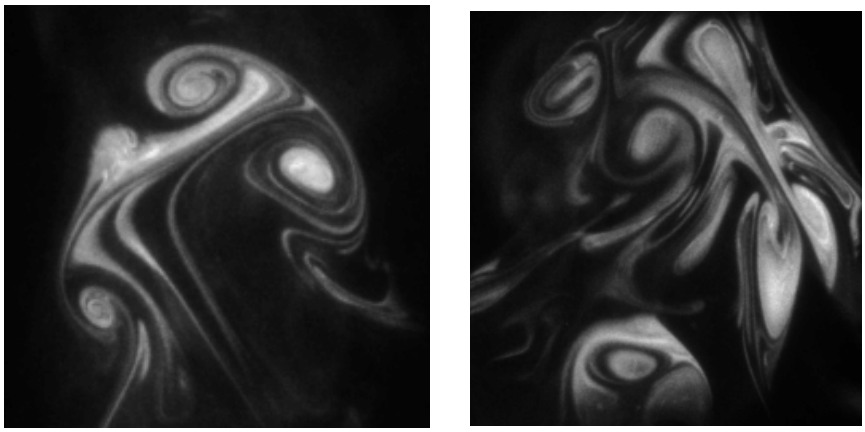

Figure 2: Sample images of instantaneous LII signal intensity (i.e. relative soot volume fraction) at a height of approximately 300 mm in the 100% O_2 flame.

3. Results and Discussion

Figure 3 shows the measured radiation intensities as a function of the flame height for the two different series of oxygen-enriched flames that were investigated. Series 1, in which the flow rate and therefore the Reynolds number of the oxidizer flow increased inversely to the concentration of oxygen in the flow, shows a significant shift downward in overall intensity and downward in flame height as the oxygen concentration decreases. There are several factors that undoubtedly contribute to the lower radiation levels with decreasing oxygen concentration: (a) decreasing flame temperature, (b) decreasing soot concentrations (see Fig. 4, and luminosity trends in Fig.

1), and (c) increasingly fast mixing of hot flame products with cooler surroundings (yielding an effective radiative quench because of the T^4 dependence of thermal radiation).

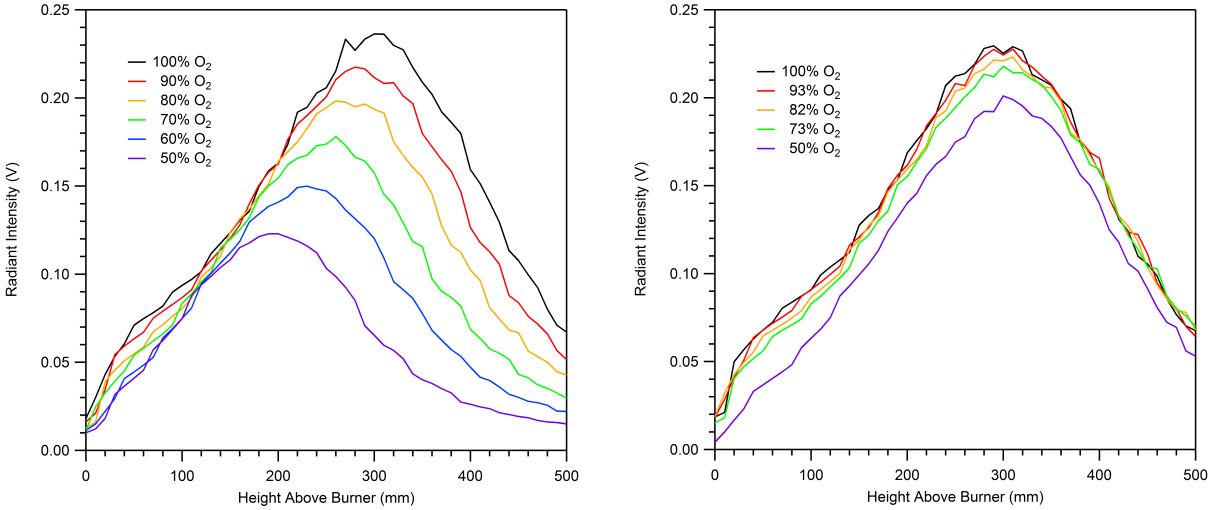

Figure 3: Centerline profiles of thermal radiation emitted from the two series of oxygen-enriched flames, with Series 1 (variable flow) to the left and Series 2 (constant flow) to the right. The radiation intensity is uncalibrated.

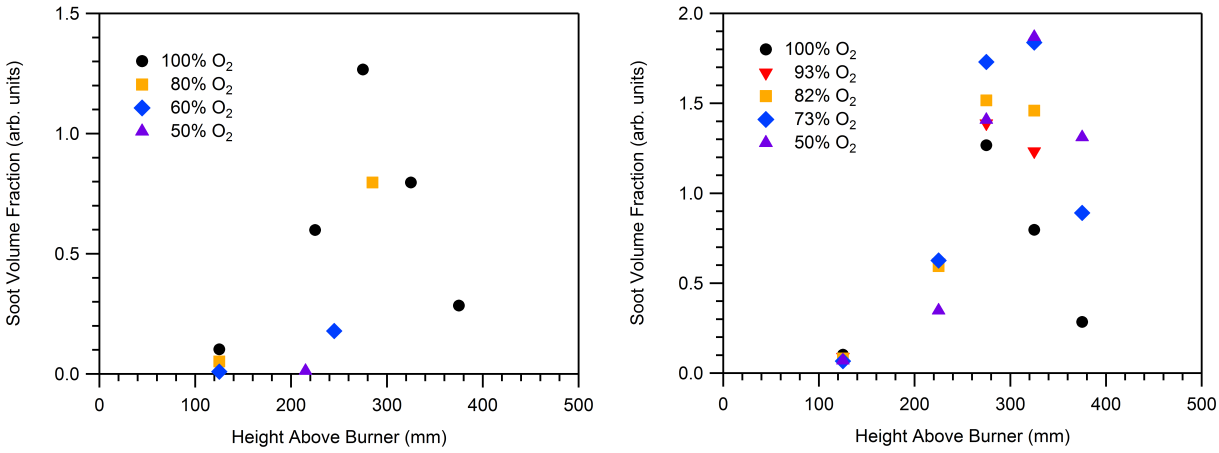

Figure 4: Centerline profiles of soot volume fraction in the two series of oxygen-enriched flames, with Series 1 (variable flow) to the left and Series 2 (constant flow) to the right. The soot volume fraction is uncalibrated.

For Series 2 flames, the radiation profile remains effectively constant for 100% O_2 decreasing down to 80% O_2. This trend is somewhat surprising, because the flame temperature is necessarily decreasing as the oxygen concentration decreases, particularly since for anything other than 100% O_2 the flame is necessarily using some ambient air to provide it with sufficient oxygen for complete fuel burnout. However, as shown in Fig. 4, the soot concentration in Series 2 is increasing somewhat as the oxygen concentration decreases, which may be providing a source of additional radiation to offset gas-phase radiation loss as the oxygen concentration decreases from

100% to 80%. Once less than 80% O_2 is used, the radiation intensity begins to fall in the Series 2 flames, but nowhere near as fast as for the Series 1 flames. Indeed, as Fig. 4 shows, while the soot formation is somewhat delayed for the 50% O_2 Series 2 flame, it ultimately reaches as high a concentration as in any of the higher O_2 flames. This factor probably accounts for the relatively small deficit in thermal radiation from the 50% O_2 Series 2 flame relative to 100% O_2.

Taken together, the radiation and soot concentration results from the two series of oxygen-enriched flames suggest that turbulent mixing has a strong effect on both soot formation and thermal radiation. Conversely, for flames that have weak enough mixing that allows for soot formation, changing the oxygen concentration from 100% down to 50% generates more soot (particularly high up in the flame) and has only a weak effect on thermal radiation from the flame. Of course, it should be understood that these trends with the Series 2 flames may reflect, in part, the effect of a substoichiometric amount of oxygen being supplied in the oxygen-enriched coannular flow. In the future, an additional series of measurements will be performed in which an excess of oxygen is always being supplied to the burner.

4. Conclusions

Preliminary measurements of soot volume fractions and thermal radiation in two different series of turbulent, non-premixed oxygen-enriched methane jet flames have demonstrated the pronounced effect of turbulent mixing intensity on soot formation and thermal radiation. For flames with lower mixing intensities and the ability to form soot, the results show only a weak dependence of thermal radiation on the oxygen concentration (from 50% to 100%) and also show similar tendencies to form soot over this wide range of oxygen concentrations. This result gives promise to the economical development of oxygen-enriched burners utilizing intermediate concentrations of oxygen that may be more economical to produce using new air separation technologies that are currently being developed. Of course, NOx emissions, which have not been characterized in this study, will increase as the oxygen purity decreases.

5. Acknowledgements

Support for this research was provided by Sandia National Laboratories' Laboratory Directed Research and Development (LDRD) program. Sandia National Laboratories is a multiprogram laboratory managed and operated by Sandia Corporation, a wholly owned subsidiary of Lockheed Martin Corporation, for U.S. DOE's National Nuclear Security Administration under contract DE-AC04-94AL85000.

6. References

[1] C.E. Baukal, Jr., Oxygen-Enhanced Combustion, 2nd Ed., Taylor & Francis Group, Boca Raton, FL, 2013.
[2] L. Chen, S.Z. Yong, A.F. Ghoniem, Progr. Energy Combust. Sci. 38 (2012) 156-214.
[3] L.M. Farrell, T.T. Pavlack, L. Rich, Iron Steel Eng. 72 (1995) 35-42.
[4] S. Grisham, Am. Glass Rev. 117 (1997) 12.
[5] J.J. Schep, "Experiences with an oxygen-fired container glass furnace with silica crown: 14 years – a world record?," 69th Conf. Glass Probs. pp. 3-11, 2009.
[6] A.R. Smith, J. Klosek, Fuel Process. Technol. 70 (2001) 115-134.
[7] W.F. Castle, Int. J. Refrig. 25 (2002) 158-172.

[8] D.M. Ruthven, S. Farooq, Gas Sep. Purif. 4 (1990) 141-148.
[9] A.M.M. Mendes, C.A.V. Costa, A.E. Rodrigues, Sep. Purif. Technol. 24 (2001) 173-188.
[10] J. Sunarso, S. Baumann, J.M. Serra, W.A. Meulenberg, S. Liu, Y.S. Lin, J.C. Diniz da Costa, J. Membrane Sci. 320 (2008) 13-41.
[11] S.M. Hashim, A.R. Mohamed, S. Bhatia, Adv. Coll. Inter. Sci. 160 (2010) 88-100.
[12] M. Eddaoudi, H. Li, O.M. Yaghi, J. Am. Chem. Soc. 122 (2000) 1391-1397.
[13] D.F. Sava Gallis, M. Parkes, J.A. Greathouse, X. Zhang, T.M. Nenoff, Chem. Mater. (2015) in press, DOI: 10.1021/cm5042293.
[14] M. Parkes, D.F. Sava Gallis, J.A. Greathouse, T.M. Nenoff, J. Phys Chem C (2015) in press, DOI: 10.1021/jp511789g.
[15] C.E. Baukal, B. Gebhart, Int. J. Heat Mass Trans. 40 (1997) 2539-2547.
[16] L. Wang, N.E. Endrud, S.R. Turns, M.D. D'Agostini, A.G. Slavejkov, Combust. Sci. Technol. 174 (2002) 45-72.